Assessment of Power Quality for Line Frequency Coreless Induction Furnaces

ANGELA IAGĂR GABRIEL NICOLAE POPA CORINA MARIA DINIŞ
Department of Electrotechnical Engineering and Industrial Informatics
Politechnica University Timişoara
Revoluției Str., no 5, Hunedoara, 331128
ROMANIA
angela.iagar@fih.upt.ro http://www.fih.upt.ro

Abstract: - This paper presents a study about power quality problems generated by line frequency coreless induction furnaces. We analyzed a furnace with 12.5 t capacity of cast-iron. The measurements have been made in the primary of the furnace transformer, on the MV line, using the CA8334 three-phase power quality analyser. Experimental results emphasized the presence of harmonics and interharmonics in the phase voltages and harmonics in the currents absorbed from the MV network. Further to harmonic analysis of the measured signals, we have been proposed some optimization methods for operation of analyzed furnace, in such way to comply with the European norms of Electromagnetic Compatibility (EMC).

Key-Words: - Power quality, Harmonics, Interharmonics, Induction furnace

1 Introduction

Today, power quality studies are becoming a growing concern [1-6].

The most important parameters which affect power quality are harmonics, voltage instability and reactive power burden [7-10]. They cause low system efficiency, poor power factor, cause disturbance to other consumers and interference in the nearly communication networks [11-15].

The increased problems in power networks impose to identify the sources of power quality deterioration.

Induction heating equipments do not introduce dust and noise emissions in operation, but cause power quality problems in the electric power system [16-18].

Induction-melt furnaces supplies by medium-frequency converters generate fixed and variable frequency harmonics [2,16,17]. Also, large furnaces operating at a few hundred hertz can generate interharmonics. Interharmonics can overload power system capacitors, introduce noise into transformers, cause lights to flicker, instigate UPS alarms, and trip adjustable-speed drives [2,16].

High-frequency systems, which operate at greater than 3 kHz are relatively small and limited to special applications. Power quality problems produced by the operation of these equipments are small.

The induction furnaces supplied at line frequency (50 Hz) are of high capacity and represent great power consumers. The operation of these furnaces also produces important disturbances in the power network.

Being single-phase loads, these furnaces introduce unbalances that lead to the increasing of power and active energy losses in the network [1,3].

Because the specialty literature does not offer detailed information regarding the harmonic distortion in the case of line frequency coreless induction furnaces, we proposed ourselves to analyze the power quality problems introduced by the operation of these furnaces.

On the other side, it must kept in view also the fact that in Romania are still operating line frequency coreless induction furnaces, and the cumulated effect of the electromagnetic pollution generated by these could be important.

2 Electrical Installation of the Analyzed Induction-Melt Furnace

It was analyzed a coreless induction furnace with 12.5 t capacity of cast-iron; the furnace is supplied from the three-phase medium-voltage network (6 kV) through a transformer in Δ/Y connection, with step-variable voltage. Load balancing of the three-phase network is currently achieved by a Steinmetz circuit, and the power factor correction is achieved by means of some step-switching capacitor banks (fig.1).

In electric diagram from fig.1: Q_1 is an indoor three-poles disconnector, type STIm–10–1250 (10 kV, 1250 A), Q_2 is an automatic circuit-breaker OROMAX (6 kV, 2500 A), T is the furnace

transformer (2625 kVA; 6/1.2 kV), K_1 is a contactor (1600 A), (1) is the symmetrization installation of three-phase network, (2) is the power factor compensation installation, TC_1, TC_2 (300/5 A) are current transformers, TT_1, TT_2 (6000/100 V) are voltage transformers, and M is the flexible connection of the induction furnace CI.

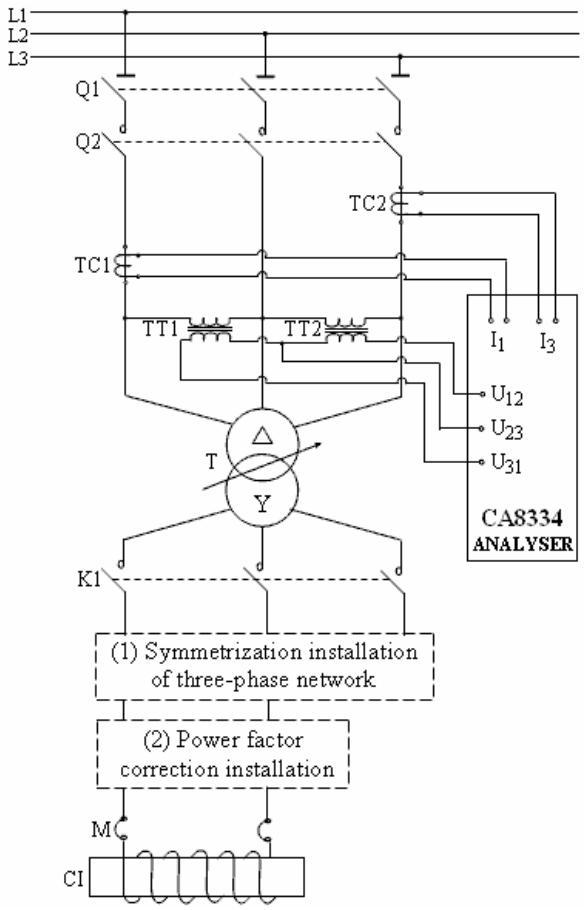

Fig.1. Experimental electric diagram

Within the study the following physical aspects were taken into account [16]:

- induction heating of ferromagnetic materials involve complex and strongly coupled phenomena (generating of eddy currents, heat transfer, phase transitions of the processed material);
- the resistivity of cast-iron increases with temperature;
- the relative magnetic permeability of the cast-iron changes very fast against temperature near to the Curie point (above the Curie temperature the cast-iron becomes paramagnetic).

As consequence, we analyzed the influence of the following factors upon the power quality of the induction furnace: the charge, the supply voltage, the symmetrization installation and the power factor correction installation.

3 Measured Signal Waveforms in Electrical Installation of the Furnace

The measurements have been made in the primary of the furnace transformer T (fig.1), using the CA8334 three-phase power quality analyser [19].

CA8334 gave an instantaneous image of the main characteristics of power quality for the analyzed induction furnace.

The main parameters measured by the CA8334 analyser were: TRMS AC phase voltages and TRMS AC line currents; peack voltage and current; active, reactive and apparent power per phase; harmonics for voltages and currents up to the 50th order.

This analyser provide numerous calculated values and processing functions in compliance with EMC standards in use (EN 50160, IEC 61000-4-15, IEC 61000-4-30, IEC 61000-4-7, IEC 61000-3-6).

The current I_2 (fig.1) was impossible to be measured because the CA8334 three-phase power quality analyser was connected to the watt-hour meter input. The watt-hour meter had three voltages (U_{12}, U_{23}, U_{31}) and two currents (I_1 and I_3).

3.1 The Cold State of the Charge

This is the first heating stage of the cast-iron charge.

The waveforms of phase voltages and currents absorbed from the network after 15 minutes from the beginning of the heating process are shown in fig.2 and fig.4. Harmonic spectra of the voltages and currents are shown in fig.3 and fig.5.

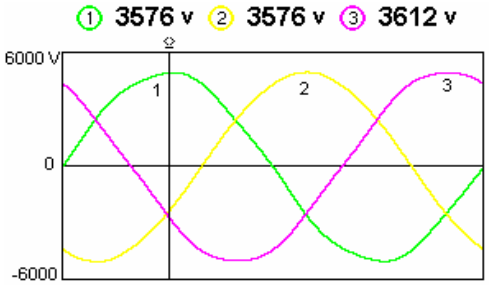

Fig.2. Phase voltages in the cold state of the charge

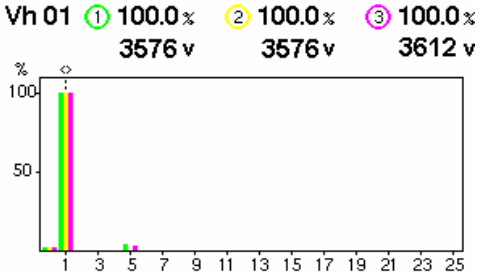

Fig.3. Harmonic spectra of the voltages in the cold state of the charge

In the first heating stage, the electromagnetic disturbances of the phase voltages are very small. The 5th harmonic is within compatibility limits [20]. Also, it can be observe the presence of interharmonics in voltages waveforms. Voltage interharmonics exceed the compatibility limits [20].

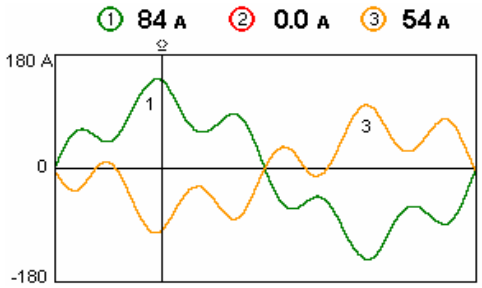

Fig.4. Line currents in the cold state of the charge

Waveform distortion of the currents in cold state is large.

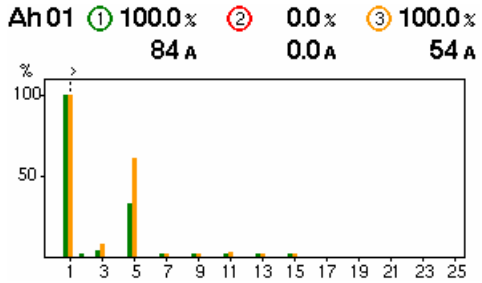

Fig.5. Harmonic spectra of the currents in the cold state of the charge

At the beginning of the cast-iron heating process the 2nd, 3rd, 5th, 7th, 9th, 11th, 13th and 15th harmonics are present in the line currents. The 5th harmonic exceeds the compatibility limits [20].

3.2 The Intermediate State of the Charge

In the intermediate state, part of the charge is heated above the Curie temperature and becomes paramagnetic, and the rest of the charge still has ferromagnetic properties. The furnace charge is partially melted.

The waveforms of phase voltages and currents absorbed from the network after 5 hours and 40 minutes from the beginning of the heating process are shown in fig.6 and fig.8. Harmonic spectra of the voltages and currents in the intermediate state of the charge are shown in fig.7 and fig.9.

In the intermediate state of the charge, phase voltages present interharmonics. Distortion of waveform is small.

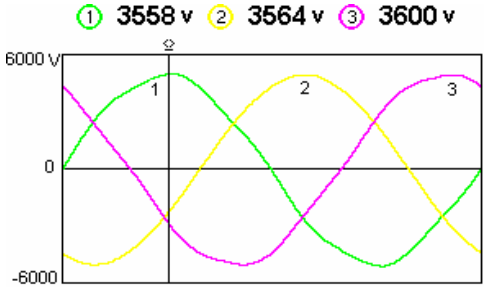

Fig.6. Phase voltages in the intermediate state

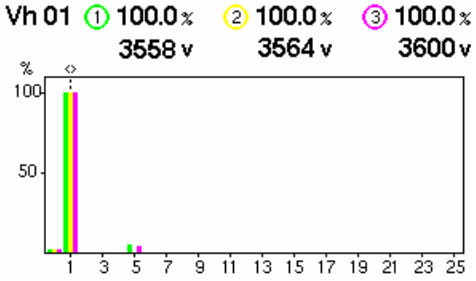

Fig.7. Harmonic spectra of the voltages in the intermediate state

In the intermediate state the 5th harmonic do not exceeds the compatibility limits, but the voltage interharmonics exceed the compatibility limits [20].

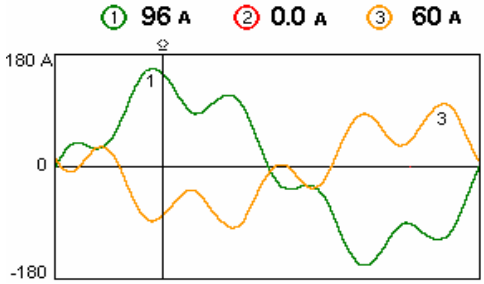

Fig.8. Line currents in the intermediate state

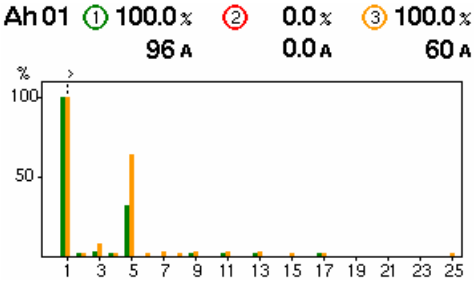

Fig.9. Harmonic spectra of the currents in the intermediate state

In the intermediate state, harmonic spectra of the currents present the 3rd, 5th, 7th, 9th, 11th, 13th, 15th, 17th, 25th harmonics and even harmonics (2nd, 4th, 6th, 8th). The 5th and 25th harmonics exceed the compatibility limits [20].

3.3 The End of the Melting Process

The furnace charge is totally melted, being paramagnetic.

The waveforms of phase voltages and currents at the end of melting (after 8 hours from the beginning of the heating process) are shown in fig.10 and fig.12.

Harmonic spectra of the voltages and currents at the end of melting are shown in fig.11 and fig.13.

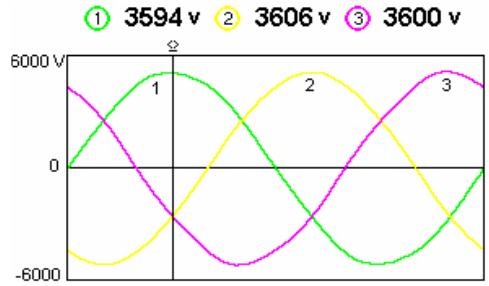

Fig.10. Phase voltages at the end of the melting process

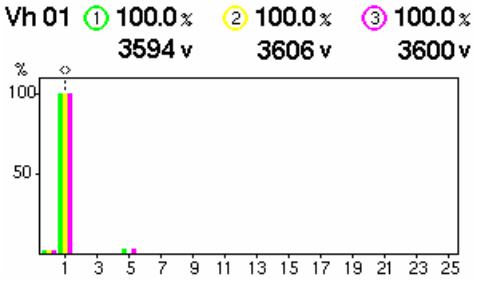

Fig.11. Harmonic spectra of the phase voltages at the end of the melting process

At the end of the melting, interharmonics are present in the phase voltages waveforms. Voltage interharmonics exceed the compatibility limits [20]. The 5th harmonic is within compatibility limits [20].

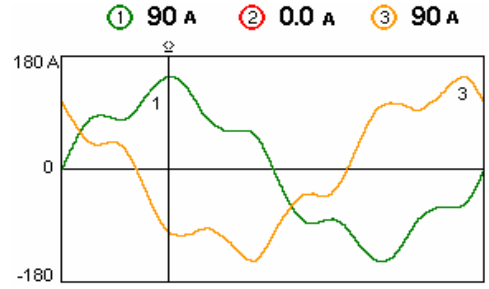

Fig.12. Line currents at the end of the melting process

Harmonic spectra of the currents at the end of the melting process show the presence of 3rd, 4th, 5th, 7th, 9th, 11th, 13th harmonics. The 5th harmonic exceeds the compatibility limits [20].

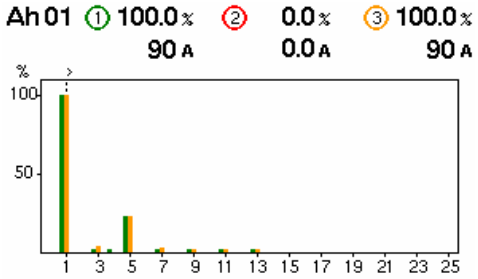

Fig.13. Harmonic spectra of the currents at the end of the melting process

4 The Values Computed by CA8334 Analyser

The values computed by the CA8334 analyser are [19]:

1. Total harmonic distortion of voltages and currents

$$V_{THD\,i} = \frac{\sqrt{\sum_{n=2}^{50} (V_{harm\,ni})^2}}{V_{harm\,1i}} \cdot 100 \quad (1)$$

$$I_{THD\,i} = \frac{\sqrt{\sum_{n=2}^{50} (I_{harm\,ni})^2}}{I_{harm\,1i}} \cdot 100 \quad (2)$$

V represents the phase voltage, I represents the line current, i represents the phase (i = 1, 2, 3) and n represents the order of harmonics.

2. Distortion factor of voltages and currents

$$V_{DF\,i} = \frac{\sqrt{\frac{1}{2}\sum_{n=2}^{50} (V_{harm\,ni})^2}}{V_{RMS\,i}} \cdot 100 \quad (3)$$

$$I_{DF\,i} = \frac{\sqrt{\frac{1}{2}\sum_{n=2}^{50} (I_{harm\,ni})^2}}{I_{RMS\,i}} \cdot 100 \quad (4)$$

V_{RMS} and I_{RMS} represent the RMS values for phase voltage and line current, computed over 1 second, and i represents the phase (i = 1, 2, 3).

3. K factor for current

$$I_{KF\,i} = \frac{\sum_{n=1}^{50} n^2 \cdot (I_{harm\,ni})^2}{\sum_{n=1}^{50} (I_{harm\,ni})^2} \quad (5)$$

In the above relation I represents the line current, i represents the phase (i = 1, 2, 3) and n represents the order of harmonics.

K factor is a weighting of the harmonic load currents according to their effects on transformer heating. A K factor of 1 indicates a linear load (no harmonics); a higher K factor indicates the greater harmonic heating effects.

4. Power factor and displacement factor

Power factor is:

$$PF_i = \frac{P_i}{S_i} \quad (6)$$

$P_i[W]$ and $S_i[VA]$ represent active power and apparent power per phase (i = 1, 2, 3).

Displacement factor is:

$$DPF_i = \cos\varphi_i \quad (7)$$

φ_i is the phase difference between the fundamental current and voltage, and i represents the phase.

5. Extreme and average values for voltage and current

MIN/MAX values for voltage (or current) represent the minimum/maximum values of the half-period RMS voltage (or current).

Peak values (PEAK+/PEAK-) for voltage (or current) represent the maximum/minimum values of the voltage (or current) for all the samples between two consecutive zeros.

Average values (AVG) for voltage and current are computed over 1 second.

6. Peak factors for current and voltage

Mathematical formulae used to compute the peak factors for current and phase voltage are:

$$V_{CFi} = \frac{\max\left(Vpp_i, |Vpm_i|\right)}{\sqrt{\frac{1}{N}\cdot\sum_{n=0}^{N-1}\left(V(n)_i\right)^2}} \quad (8)$$

$$I_{CFi} = \frac{\max\left(Ipp_i, |Ipm_i|\right)}{\sqrt{\frac{1}{N}\cdot\sum_{k=0}^{N-1}\left(I(k)_i\right)^2}} \quad (9)$$

In the relations (8)-(9):

- Vpp is the PEAK+ of the phase voltage;
- Vpm is the PEAK- of the phase voltage;
- Ipp is the PEAK+ of the line current;
- Ipm is the PEAK- of the line current;
- i represents the phase (i = 1, 2, 3);
- N represents the number of the samples per period (between two consecutive zeros).

For a sinusoidal signal, the peak factor is equal to $\sqrt{2}$ (1.41).

For a non-sinusoidal signal, the peak factor can be either greater than or less than $\sqrt{2}$. In the latter case, the peak factor signals divergent peak values with respect to the RMS value.

Tables 1-13 show the computed values by CA8334 analyser on MV network.

Tables 1 and 2 show the total harmonic distortion for phase voltages and for line currents in all the heating stages.

Table 1
Total harmonic distortion THD [%] for phase voltages

Heating moment	u_1	u_2	u_3
Cold state	2.2	0	1.7
Intermediate state	3.4	0	3.1
End of melting process	1.9	0	1.7

THD of phase voltages do not exceed the compatibility limits on MV network in all the heating stages.

Table 2
Total harmonic distortion THD [%] for line currents

Heating moment	i_1	i_3
Cold state	31	57.5
Intermediate state	34.3	68.7
End of melting process	22.7	24.3

THD of line currents exceed the limits permitted by norms in all the analyzed situations.

Because THD of line currents exceed 20%, this indicates a significant electromagnetic pollution produced by the analyzed furnace in MV network.

Tables 3 and 4 show the distortion factor for phase voltages and for line currents in all the heating stages.

Table 3
Distortion factor DF [%] of phase voltages

Heating moment	u_1	u_2	u_3
Cold state	1.9	0	1.4
Intermediate state	3.4	0	3
End of melting process	1.9	0	1.4

Distortion factor of phase voltages is smaller than

total harmonic distortion in all the situations.

Table 4
Distortion factor DF [%] of line currents

Heating moment	i_1	i_3
Cold state	23.9	43.2
Intermediate state	32.2	61.8
End of melting process	22.7	23.4

Distortion factor of line currents is very high in all the analyzed situations.

Table 5
K factor KF [-] of line currents

Heating moment	i_1	i_3
Cold state	2.51	5.59
Intermediate state	3.54	8.7
End of melting process	2.21	2.27

In all the heating stages K factor is greater than unity.

The values of K factor in the cold state and in intermediate state are very high and indicate the significant harmonic current content. K factor decrease at the end of the melting. Harmonics generate additional heat in the furnace transformer. If the transformer is non-K-rated, overheat possibly causing a fire, also reducing the life of the transformer.

Tables 6-8 show the extreme and average values for phase voltages in all the heating stages.

Table 6
Extreme and average values for phase voltages in cold state

Values	u_1	u_2	u_3
MAX [V]	4176	4182	4158
AVG [V]	3558	3564	3600
MIN [V]	0	2862	2796
PEAK+ [V]	5034	5058	5028
PEAK- [V]	-5076	-5076	-5046

Table 7
Extreme and average values for phase voltages in intermediate state

Values	u_1	u_2	u_3
MAX [V]	4176	4092	4194
AVG [V]	3552	3558	3588
MIN [V]	3456	3324	3432
PEAK+ [V]	5076	5034	5028
PEAK- [V]	-5118	-5076	-5064

Table 8
Extreme and average values for phase voltages at the end of melting

Values	u_1	u_2	u_3
MAX [V]	4140	4068	4146
AVG [V]	3594	3606	3600
MIN [V]	3558	3522	3480
PEAK+ [V]	5052	5118	5028
PEAK- [V]	-5094	-5136	-5046

The extreme and average values of phase voltages indicate a small unbalance in all the analyzed situations. Peak values (PEAK+/PEAK-) of phase voltages are not very high (comparatively with the maximum values) during the heating stages of the cast-iron.

Tables 9-11 show the extreme and average values for line currents in all the heating stages.

Table 9
Extreme and average values for line currents in cold state

Values	i_1	i_3
MAX [A]	96	60
AVG [A]	84	48
MIN [A]	0	0
PEAK+ [A]	138	90
PEAK- [A]	-138	-90

Table 10
Extreme and average values for line currents in intermediate state

Values	i_1	i_3
MAX [A]	324	240
AVG [A]	96	60
MIN [A]	0	0
PEAK+ [A]	162	108
PEAK- [A]	-162	-102

Table 11
Extreme and average values for line currents at the end of melting

Values	i_1	i_3
MAX [A]	102	102
AVG [A]	90	90
MIN [A]	90	84
PEAK+ [A]	150	150
PEAK- [A]	-150	-150

The extreme and average values of line currents indicate a large unbalance in cold state and in intermediate state. At the end of melting the unbalance is small.

Maximum values of line currents are very high during the intermediate state.

Tables 12 and 13 show the values of peak factors

in all the heating stages.

Table 12
Peak factors CF [-] of phase voltages

Heating moment	u_1	u_2	u_3
Cold state	1.42	1.42	1.39
Intermediate state	1.44	1.42	1.39
End of melting process	1.45	1.47	1.49

Peak factors of phase voltages are very close to the peak factor for sinusoidal signals (1.41) in all the heating stages. This indicates a small distortion of phase voltages in MV network.

Table 13
Peak factors CF [-] of line currents

Heating moment	i_1	i_3
Cold state	1.68	1.82
Intermediate state	1.72	1.79
End of melting process	1.68	1.68

Peak factors of line currents are between 1.68 and 1.82. A high peak factor characterizes high transient overcurrents which, when detected by protection devices, can cause nuisance tripping.

Fig.14-17 show the recorded parameters (total harmonic distortion of phase voltages and currents - V_{THD}, I_{THD}; power factor and diplacement factor per phase 1 - PF, DFP) in the first stage of the heating. Total recording period was 11:20-12:18.

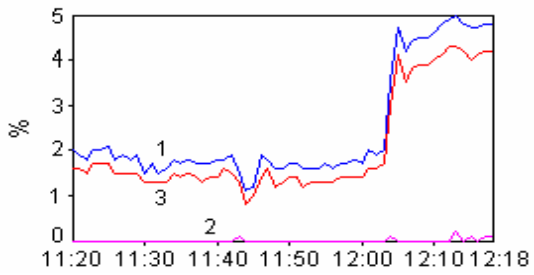

Fig.14. Recorded values of V_{THD} in the cold state

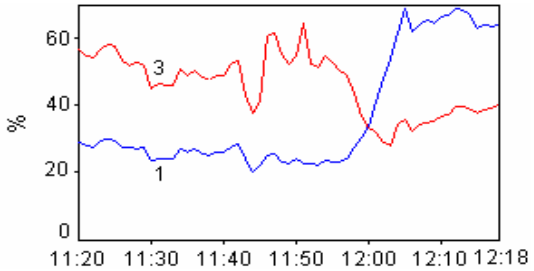

Fig.15. Recorded values of I_{THD} in the cold state

In the recording period of cold state, THD of phase voltages are within compatibility limits, but THD of line currents exceed the compatibility limits.

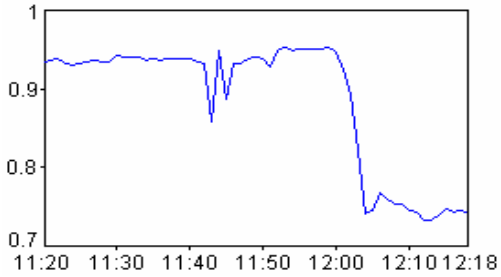

Fig.16. Recorded values of PF per phase 1 in the cold state

In the first stage of the heating PF per phase 1 is less than unity; in the time period 12:00 - 12:18 PF is less than neutral value (0.92).

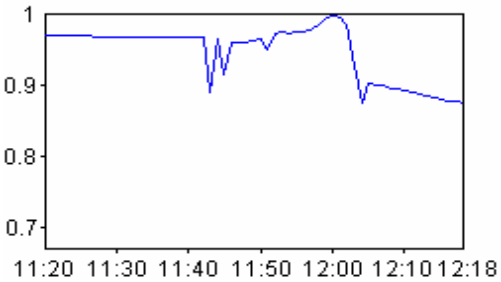

Fig.17. Recorded values of DPF per phase 1 in the cold state

In the recording period, displacement factor per phase 1 is less than unity, but exceeds the values of power factor per phase 1.

Fig.18-21 show the recorded parameters in the intermediate state of the heating.

The furnace charge was partially melted in the recording period, 13:20-14:18.

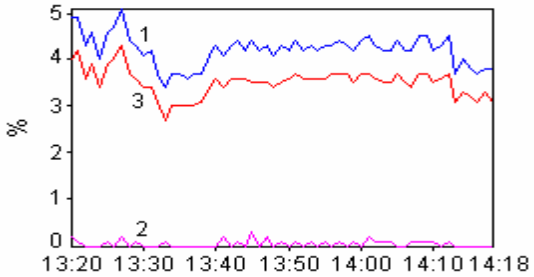

Fig.18. Recorded values of V_{THD} in the intermediate state

In the intermediate state, THD of phase voltages do not exceed the compatibility limits, but are bigger comparatively with cold state.

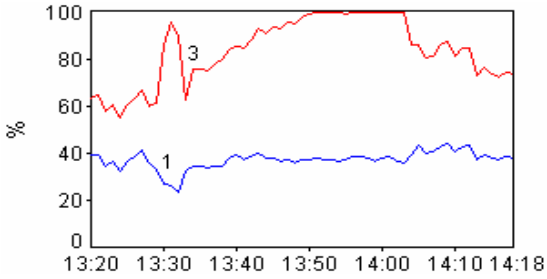

Fig.19. Recorded values of I_{THD} in the intermediate state

THD of line currents are remarkably high in intermediate state and exceed the compatibility limits.

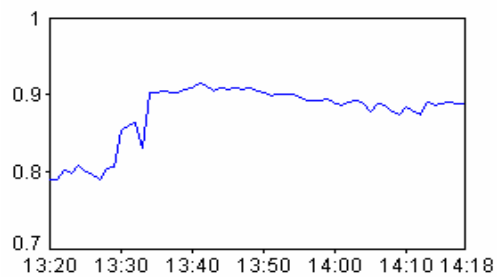

Fig.20. Recorded values of PF per phase 1 in the intermediate state

PF per phase 1 is less than unity, and in the time period 13:20-13:35, PF is less than neutral value (0.92).

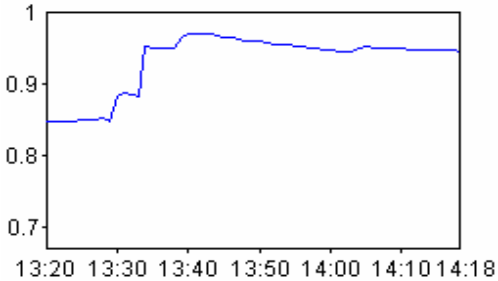

Fig.21. Recorded values of DPF per phase 1 in the intermediate state

Displacement factor per phase 1 is less than unity in the recording period of intermediate state.

In the time period 13:20-13:35, DPF is less than neutral value (0.92). DPF exceeds the values of power factor PF per phase 1.

Fig.22-25 show the recorded parameters in the last stage of the heating.

The furnace charge was totally melted in the recording period, 18:02-18:12.

In the last stage of the melting process, THD of phase voltages are within compatibility limits, being smaller comparatively with cold state or intermediate state.

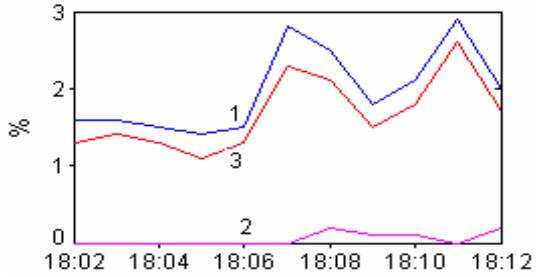

Fig.22. Recorded values of V_{THD} in the last stage of the melting process

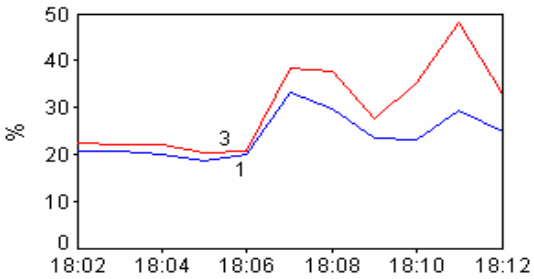

Fig.23. Recorded values of I_{THD} in the last stage of the melting process

THD of line currents are smaller comparatively with cold state or intermediate state, but exceed the compatibility limits.

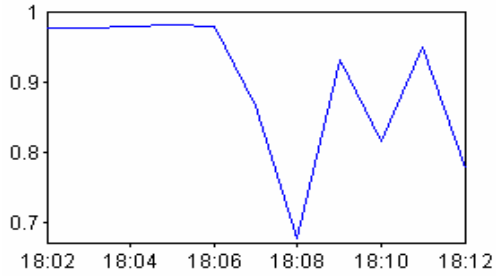

Fig.24. Recorded values of PF per phase 1 in the last stage of the melting process

In the last stage of the melting process PF per phase 1 is less than unity. In the time period 18:06-18:12, PF is less than neutral value (0.92).

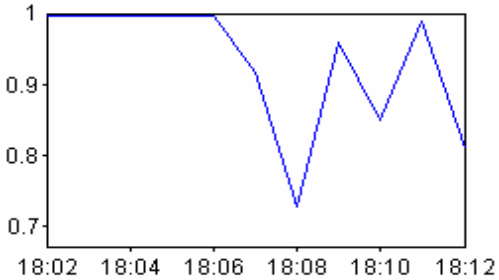

Fig.25. Recorded values of DPF per phase 1 in the last stage of the melting process

Displacement factor per phase 1 is less than unity in the time period 18:06-18:12. DPF values exceed the values of power factor PF per phase 1.

Under nonsinusoidal conditions, any attempt to achieve unity PF does not result in harmonic-free current. Similarly, compensation for current harmonics does not yield unity PF. The best solution to this tradeoff is the optimization of PF, THD and SHD (specific harmonic distortion) [21,22].

5 Conclusions

The measurements results show that the operation of the analyzed furnace determines interharmonics and harmonics in the phase voltages and harmonics in the currents absorbed from the network.

THD of phase voltages are within compatibility limits, but voltage interharmonics exceed the compatibility limits in all the analyzed situations.

THD of line currents exceed the compatibility limits in all the heating stages.

Because I_{THD} exceed 30%, which indicates a significant harmonic distortion, the probable malfunction of system components would be very high.

THD of line currents are bigger in intermediate state comparatively with cold state, or comparatively with the end of melting.

This situation can be explained by the complex and strongly coupled phenomena (eddy currents, heat transfer, phase transitions) that occur in the intermediate state.

Harmonics can be generated by the interaction of magnetic field (caused by the inductor) and the circulating currents in the furnace charge.

In the case of currents, 5^{th} and 25^{th} harmonics exceed the compatibility limits.

To reduce the heating effects of harmonic currents created by the operation of analyzed furnace it must replaced the furnace transformer by a transformer with K-factor of an equal or higher value than 4.

Peak factors of line currents are between 1.68 and 1.82 during the heating stages. This high peak factor characterizes high transient overcurrents which, when detected by protection devices, can cause nuisance tripping.

The capacitors for power factor correction and the ones from Steinmetz circuit amplify in fact the harmonic problems.

PF is less than unity in all the analyzed situations. But, Steinmetz circuit is efficient only for unity PF, under sinusoidal conditions [16].

For optimizing the operation of analyzed induction furnace, it's imposing the simultaneous adoption of three technical measures: harmonics filtering, reactive power compensation and load balancing.

That is why harmonic filters must be introduced in the primary of furnace transformer to solve the power quality problems.

In order to eliminate the unbalance, we suggest to add another symmetrization system in the connection point of the furnace to the power supply network.

Acknowledgments:

This research has done by a grant research support. This project has been selected and funded by the BALKAN ENVIRONMENTAL ASSOCIATION (B.EN.A.), with the COSMOTE-ROMANIA sponsorship funds.

References:

[1] J. Arrillaga, N. R. Watson, S. Chen, *Power System Quality Assessment*, New York, John Wiley and Sons, 2000.

[2] F. C. de la Rosa, *Harmonics and Power Systems,* CRC Press, Taylor&Francis Group, 2006.

[3] F. Lattarulo (Editor), *Electromagnetic Compatibility in Power System*, Elsevier Science&Technology Books, 2006.

[4] F. Muzi, Real-time Voltage Control to Improve Automation and Quality in Power Distribution, *WSEAS Transactions on Circuit and Systems,* Vol. 7, Issue 1, 2008, pp.173-183.

[5] F. Muzi, L. Passacantando, Improvements in Power Quality and Efficiency with a New AC/DC High Current Converter, *WSEAS Transactions on Circuit and Systems,* Vol. 7, Issue 5, 2008, pp.338-347.

[6] S. G. Seifossadat, M. Razzaz, M. Moghaddasian, M. Monadi, Harmonic Estimation in Power Systems Using Adaptive Perceptrons Based on a Genetic Algorithm, *WSEAS Transactions on Power Systems,* Vol. 2, Issue 11, 2007, pp.239-244.

[7] M. Popescu, A. Bitoleanu, M. Dobriceanu, Harmonic Current Reduction in Railway Systems, *WSEAS Transactions on Systems,* Vol. 7, Issue 7, 2008, pp.689-698.

[8] C. Panoiu, I. Baciu, M. Panoiu, C. Cuntan, Simulation Results on the Currents Harmonics Mitigation on the Railway Station Line Feed using a Data Acquisition System, *WSEAS Transactions on Electronics,* Vol. 4, Issue 10, 2007, pp.227-236.

[9] M. Panoiu, C. Panoiu, M. Osaci, I. Muscalagiu, Simulation Result about Harmonics Filtering Using Measurement of Some Electrical Items in Electrical Installation on UHP EAF, *WSEAS Transactions on Circuit and Systems,* Vol. 7, Issue 1, 2008, pp.22-31.

[10] Yang Han, Gang Yao, Li-Dan Zhou, Chen Chen, Harmonic Mitigation of Residential Distribution System using a Novel Hybrid Active Power Filter, *WSEAS Transactions on Power Systems,* Vol. 2, Issue 12, 2007, pp.255-260.

[11] W. Hosny, B. Dobrucky, Harmonic Distortion and Reactive Power Compensation in Single Phase Power Systems using Orthogonal Transformation Strategy, *WSEAS Transactions on Power Systems,* Vol. 3, Issue 4, 2008, pp.237-246.

[12] Sudhir Sharma, K.S. Sandhu, Role of Reactive Power Source on Power Quality of Three-Phase Self-Excited Induction Generator, *WSEAS Transactions on Power Systems*, Vol. 3, Issue 4, 2008, pp.216-225.

[13] A. Ghasemi, S. S. Mortazavi, R. Kianinezhad, Fuzzy Logic Controlled Adaptive Active Power Filter for Harmonics Minimization and Reactive Power Compensation under Fast Load Variation, *WSEAS Transactions on Power Systems*, Vol. 3, Issue 5, 2008, pp.300-309.

[14] Ching-Tzong Su, Chen-Yi Lin, Ji-Jen Wong, Optimal Size and Location of Capacitors Placed on a Distribution System, *WSEAS Transactions on Power Systems,* Vol. 3, Issue 4, 2008, pp.247-256.

[15] H. Tatizawa, E. S. Neto, G. F. Burani, A. A. C. Arruda, K. T. Soletto, N. M. Matsuo, Application of Modelling and Computer Simulation for the Development of a Test Setup for Calibration of Power Quality Measurement Transducers for High Voltage Networks, *WSEAS Transactions on Systems,* Vol. 7, Issue 9, 2008, pp.880-889.

[16] V. Rudnev, D. Loveless, R. Cook, M. Black, *Handbook of Induction Heating,* CRC Press, Taylor&Francis Group, 2002.

[17] ***, Power Quality for Induction Melting in Metal Production, *TechCommentary Electric Power Research Institute,* U.S.A., 1999.

[18] J. Nuns, H. Foch, M. Metz, X. Yang, Radiated and Conducted Interferences in Induction Heating Equipment: Characteristics and Remedies, *Fifth European Conference on Power Electronics and Applications,* Vol.7, 1993, pp.194-199.

[19] ***, *CA8334*, *Three Phase Power Quality Analyser*, technical handbook, Chauvin Arnoux, France, 2007.

[20] ***, IEC/TR 61000-3-6, EMC, Part 3-6: Limits – *Assessment of Harmonic Emission Limits for the Connection of Distorting Installations to MV, HV and EHV Power Systems* (revision), 2005.

[21] S. George, V. Agarwal, Optimum Control of Selective and Total Harmonic Distortion in Current and Voltage Under Nonsinusoidal Conditions, *IEEE Transactions on Power Delivery,* Vol.23, Issue 2, 2008, pp.937-944.

[22] T.B Sekara, J.C. Mikulovic, Z.R. Djurisic, Optimal Reactive Compensators in Power Systems Under Asymmetrical and Nonsinusoidal Conditions, *IEEE Transactions on Power Delivery*, Vol.23, Issue 2, 2008, pp.974-984.